Spectral-Domain Optical Coherence Tomography with an Arrayed Waveguide Grating Spectrometer

V. Duc. Nguyen,[1] B. I. Akca,[2] K. Wörhoff,[2] R. M. de Ridder,[2] M. Pollnau,[2] T. G. van Leeuwen,[1,3] J. Kalkman[1]

[1] *Biomedical Engineering & Physics University of Amsterdam, Academic Medical Center, , Amsterdam, 1100 DE, The Netherlands.*

[2]*Integrated Optical MicroSystems Group, MESA+ Institute for Nanotechnology, University of Twente, 7500 AE Enschede, The Netherlands.*

[3] *Biomedical Photonic Imaging, MIRA Institute for Biomedical Technology & Technical Medicine, University of Twente, P.O. Box 217, 7500 AE Enschede, The Netherlands.*

e-mail: *d.v.nguyen@amc.uva.nl*

Abstract: We designed and fabricated an arrayed waveguide grating (AWG) in silicon oxynitride as spectrometer for optical coherence tomography (OCT). The AWG is used as a spectrometer in a fiber-based SD-OCT system. OCT measurements are performed and demonstrate imaging up to the maximum imaging depth of 1 mm at a spatial resolution of 19-μm. Finally, an OCT image was made of a multi-layered phantom using the AWG-based SD-OCT system.

1. Introduction

Optical coherence tomography (OCT) [1] is an interferometric imaging technique which has been developed in the last 20 years. It generates high resolution cross-sectional images up to a few millimeters deep. Nowadays OCT is gaining widespread use in the clinic, particularly in ophthalmology. However, current OCT systems generally are bulky and expensive. Integrated optics is expected to make OCT system significantly smaller and more cost efficient [2-5].

In spectral-domain OCT (SD-OCT), one of the key components is the spectrometer where light is diffracted and dispersed via diffraction gratings. In integrated optics, the arrayed waveguide grating (AWG), first proposed by Smit in 1988 [6], was designed and used as a dispersive element in telecommunications for wavelength division multiplexing. With its high resolution and compactness, AWG spectrometers provide an excellent performance SD-OCT. We design an AWG spectrometer with large bandwidth in silicon-oxynitride (SiON) as a spectrometer for SD-OCT. SiON is transparent over a long wavelength range that covers all the frequently used OCT wavelength bands at 800, 1000, and 1300 nm. We perform OCT characterization and imaging with a SiON-based AWG spectrometer designed for 1300 nm center wavelength and use it in a fiber based SD-OCT system. To the best of our knowledge, this is the first time an AWG spectrometer was employed in OCT and used for optical imaging.

2. Materials and Methods

2.1 Arrayed waveguide grating spectrometer (AWG) design

The AWG structure includes input waveguide, output waveguide, free propagation regions (FPR), object plane, image plane and arrayed waveguides as illustrated in the inset in Fig. 1. The operation principle of AWG is as follows: light is transmitted into the input waveguide where it enters the first FPR; the light diverges and is then coupled into the arrayed waveguides. The length difference between the adjacent waveguides in the arrayed waveguide is chosen to be an integer number of the central wavelength. With this choice, the wave-front at the beginning of the second FPR is cylindrical and causes light focused on the image plane [6].

For this AWG spectrometer, we aim at an 18-μm depth resolution (calculated based on the transmission spectrum of the AWG spectrometer) and 1-mm depth range determined by the wavelength resolution $\delta\lambda$ (wavelength spacing per output waveguide). These requirement necessitate a large free spectral range (FSR = 78 nm) and high wavelength resolution ($\delta\lambda$ = 0.4 nm) of the AWG spectrometer.

Single-mode silicon oxynitride (SiON) channel waveguides with 2 μm width and 0.8 μm height were used for the AWG spectrometer. For the upper cladding a 4-μm-thick silicon dioxide layer was used. The core and cladding refractive indices were 1.55 and 1.45 at 1.3 μm, respectively. The minimum bending radius of curved waveguides was calculated to be 500 μm. The minimum spacing between the arrayed waveguides and between the 195 output waveguides were optimized using the beam propagation method in order to reduce loss and crosstalk values [7].

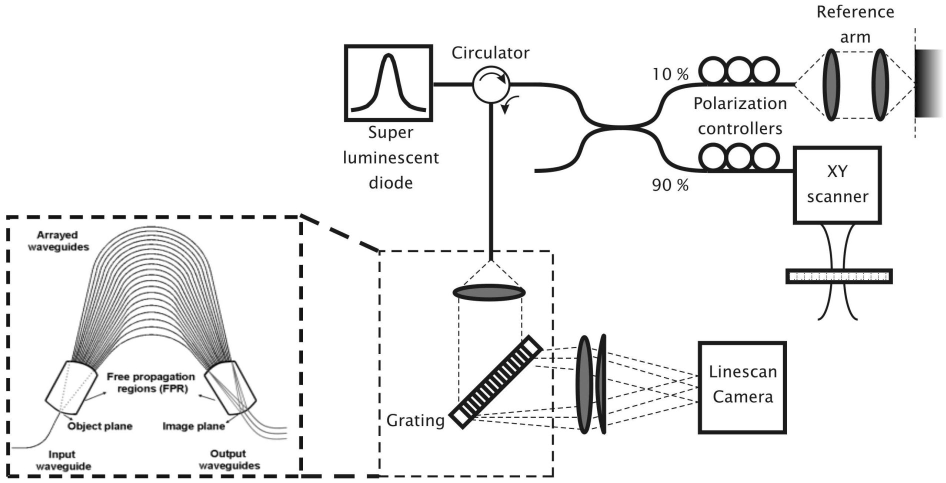

Fig. 1 Schematic of the experimental setup used for fiber-based SD OCT with an AWG spectrometer.

2.2 Experiment

A schematic of the fiber-based SD-OCT system with AWG spectrometer is shown in Fig. 1. The Michelson interferometer was illuminated with a superluminescent diode which had a partially-polarized Gaussian-like spectrum of 40-nm bandwidth and a central wavelength of 1300-nm. Via a circulator the light was coupled into a 90/10 beam splitter. Polarization controllers were placed into both, sample and reference arm. The backreflected light was redirected through the optical circulator to the spectrometer. The diffraction grating, which is commonly used in this SD-OCT system [8], was replaced by the integrated AWG. The beam coming out from output waveguides of AWG was focused onto a 46 kHz CCD linescan camera using a high numerical aperture camera lens. A moveable mirror was placed in the sample arm to measure signals in depth.

The acquired spectra are processed by first subtracting the reference arm spectrum, then compensating the dispersion, and finally re-sampling to k-space. The obtained spectrums were Fourier transformed to obtain the OCT signal. The reference spectrum, which is the transmission spectrum of the AWG spectrometer, was used to calculate the theoretical axial resolution [9].

3. Results

Figure 2 shows the reference spectrum and the interference spectrum after reference subtraction at 100-µm depth. The theoretical axial resolution calculated based on the reference spectrum is 18-µm.

The OCT signals in depth measured are shown in Fig. 3. The (maximum) depth range is calibrated using the wavelength spacing $\delta\lambda$ from the AWG as input. We are able to achieve an OCT imaging up to the maximum depth range of 1 mm. The ratio of the spectral resolution to the sampling interval ω, [10] determined from the signal decay data in Fig 3, is ω=1.2. The measured signal-to-noise ratio was 75 dB at 100 micrometer depth.

Fig. 4 shows the measured axial resolution (full width at half maximum) in depth in comparison with the theoretical axial resolution (18-µm). A slight decrease in depth resolution is observed at larger depths, which may be due to lens aberration from the imaging system

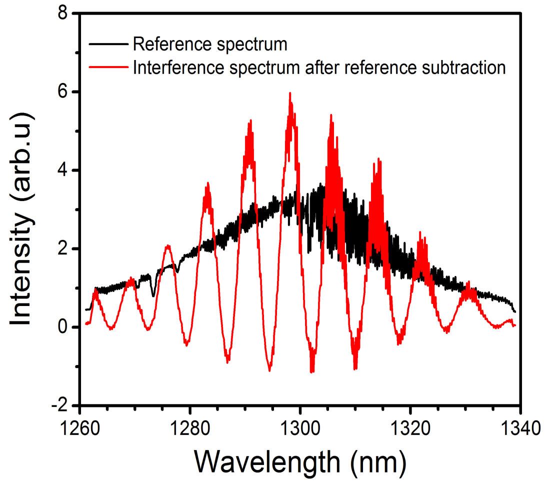

Fig. 2 Reference spectrum (black line) and interference spectrum after reference spectrum subtraction (red line).

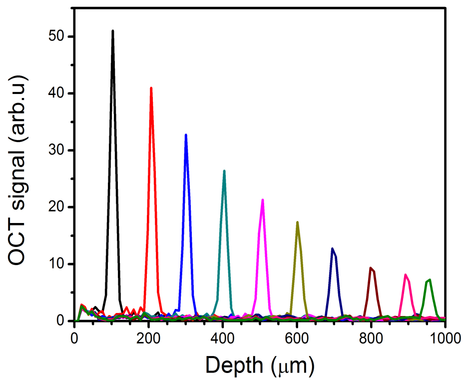

Fig. 3 OCT magnitude in depth for a mirror in the sample arm.

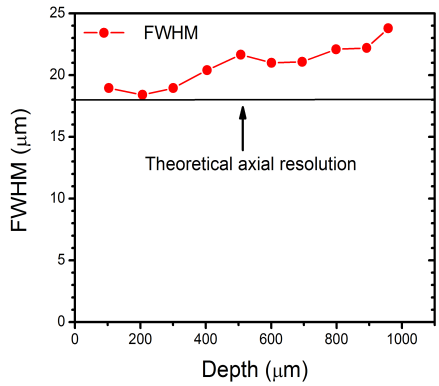

Fig. 4: Measured OCT axial resolutions (red) with the AWG in comparison with the theoretical axial resolution.

As a demonstration of OCT imaging using the AWG spectrometer, an image of a layered phantom is shown in Fig. 5 and was obtained by scanning the sample arm beam over the sample. The phantom consists of three layers of scattering medium (μ_s = 4 mm^{-1}, refractive index n = 1.41) interleaved with non-scattering tape. We can observe all three scattering layers up to the maximum imaging depth of 1 mm. The current imaging resolution and imaging depth are sufficient for biological imaging but can be increased by increasing the FSR and the number of output channels.

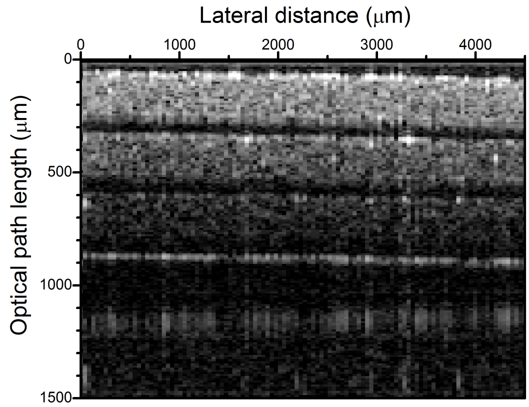

Fig. 5 An OCT image of the layered phantom measured with the AWG as spectrometer

4. Conclusions

We have demonstrated the first partially integrated SD-OCT system by designing a SiON-based AWG spectrometer for the 1300-nm spectral region. An imaging depth of 1 mm and an axial resolution of 19 μm (at 100 μm depth) were obtained. OCT imaging of a layered scattering phantom was demonstrated.

5. References

[1] D. Huang, E. A. Swanson, C. P. Lin, J. S. Schuman, W. G. Stinson, W. Chang, M. R. Hee, T. Flotte, K. Gregory, C. A. Puliafito, and J. G. Fujimoto, "Optical coherence tomography," Science **254**, 1178-1181 (1991).

[2] D. Culemann, A. Knuettel, and E. Voges , "Integrated optical sensor in glass for optical coherence tomography," IEEE J. Select. Topics Quantum Electron. **5**, 730-734 (2000).

[3] E. Margallo-Balbas, M. Geljon, G. Pandraud, and P. J. French, "Miniature 10 kHz thermo-optic delay line in silicon," Opt. Lett. **35**, 4027-4029 (2010).

[4] G. Yurtsever and R. Baets, "Towards integrated optical coherence tomography system on silicon on insulator," Proceedings of the Optical Coherence Tomography and Coherence Domain Optical Methods in Biomedicine XIV, Proc. SPIE **7554**, 1605-7422 (2010).

[5] V. D. Nguyen, N. Ismail, F. Sun, K. Wörhoff, T. G. van Leeuwen, and J. Kalkman, "SiON integrated optics elliptic couplers for Fizeau-based optical coherence tomography," J. of Lightw. Technol. **28**, 2836 (2010).

[6] M. K. Smit and C. van Dam, "PHASAR-based WDM-devices: Principles, design and applications," IEEE J. Select. Topics Quantum Electron. **2**, 236–250 (1996).

[7] B. I. Akca, N. Ismail, G. Sengo, F. Sun, J. Kalkman, A. Driessen, M. Pollnau, K. Wörhoff, and R. M. de Ridder, "High-resolution silicon-oxynitride arrayed waveguide grating spectrometers operating around 800 nm and 1300 nm", Submitted.

[8] J. Kalkman, A. V. Bykov, D. J. Faber, and T. G. van Leeuwen "Multiple and dependent scattering effects in Doppler optical coherence tomography"; Opt. Expr. **18**, 3883 (2010).

[9] Arnaud Dubois, Laurent Vabre, Albert-Claude Boccara, and Emmanuel Beaurepaire, "High-resolution full-field optical coherence tomography with a Linnik microscope", Appl. Opt. **41**, 805 (2002).

[10] N. A. Nassif *et al.*, "In vivo high-resolution video-rate spectral-domain optical coherence tomography of the human retina and optic nerve," Opt. Expr. **12**, pp. 367, 2004.